Solution Studies of $Re^{V}O$(*anti*-D-penicillaminato-*N,S,O*)(*syn*-D-penicillaminato-*N,S*)

Lory Hansen,[†] Xiaolong Xu,[†] Kwok To Yue,[‡] Zsuzsanna Kuklenyik,[§] Andrew Taylor, Jr.,[†] and Luigi G. Marzilli*[,§]

Departments of Radiology, Chemistry, and Physics, Emory University, Atlanta, Georgia 30322

Received August 2, 1995[⊗]

The known Re(V)=O complex of D-penicillamine (D-penH$_4$; the subscript indicates the number of dissociable protons) is isolated as a neutral form, ReO(D-penH$_3$)(D-penH$_2$) (**1**). The complex is six-coordinate with one CO_2^- bound *trans* to the oxo ligand, resulting in a *cis*-N_2, *cis*-S_2, *trans*-O_2 geometry. One carboxyl group is *anti* and the other is *syn* to the oxo ligand; only the *anti*-pen CO_2^- can coordinate. For **1**, in high-pH solutions, we have found unusual ^{1}H NMR spectral properties that have led to the discovery of a facile oxo ligand exchange process. **1** was also studied by acid−base titration, which revealed that the neutral-pH form (**I**) was [ReO(*syn*-D-penH$_2$-*N,S*)(*anti*-D-penH$_2$-*N,S,O*)]$^-$. Significant spectroscopic changes occurred at pH ∼11 and above. The *two* sets of pen ^{1}H NMR signals observed at neutral pH decreased in intensity as the pH was raised, and several original signals shifted. Simultaneously, *one* new set of pen signals emerged. These new signals also shifted with increasing pH. These results indicate that (a) form **I** is in fast equilibration with a deprotonated form (**I′**), (b) this mixture is in slow equilibrium with forms having different characteristics (**II** and **II′**), and (c) **II** and **II′** rapidly interconvert. The **II**/**II′** component has one set of pen signals. Acid−base titrations indicated that the conversions from form **I** to forms **I′** and **II** each involve consumption of 1 mol of OH^-. The nature of the forms present at different pH's was also examined by resonance Raman, UV−visible, and circular dichroism (CD) spectroscopy. These methods indicate OH^- converts **I** into an equilibrium mixture: **I′** (by deprotonation of one NH) and **II** (by displacement of the axial carboxyl by axial hydroxo). An additional equivalent of OH^- converted these two forms to **II′**, which is probably a *trans*-dioxo species. Under conditions in which **I′**, **II**, and **II′** coexisted, only the last two interconverted rapidly on the NMR time scale, since they interconverted by addition or loss of a proton. **I′** can convert to **II** only by a slower deligation process. **II** and **II′** were readily distinguished by the Raman experiment but not the longer time scale NMR experiments. Results in methanol supported this interpretation and only **I**, **I′**, and $\mathbf{II}_{MeOH}$ were formed. $\mathbf{II}_{MeOH}$ differs from **II** in having an axial methoxo ligand. The methoxo ligand cannot be converted to an oxo ligand; thus, no **II′** was observed in methanol, and the NMR spectrum of $\mathbf{II}_{MeOH}$ has *two* sets of pen signals. The one set of pen signals for **II** in water can be explained by facile proton exchange interconverting the axial hydroxo/oxo and oxo/hydroxo sites.

Introduction

Bis(aminoethanethiol) (BAT) (or diamino−dithiol (DADT)) complexes of $[Tc^{V}O]^{3+}$ and $[Re^{V}O]^{3+}$ comprise an important class of compounds in radiopharmaceutical chemistry. The BAT ligands are nonmacrocyclic quadridentate compounds that coordinate to the metal through two terminal deprotonated thiol groups and two amino groups, forming three chelate rings (Chart 1). ^{99m}TcO(BAT) complexes and bioconjugates are promising agents for imaging kidney function,[1,2] brain perfusion,[3] heart perfusion[4] and for tumor localization.[5] Re analogs have been important in the characterization of the Tc systems[6−9] and are potential $^{186/188}$Re radiotherapeutic agents.[5,10]

As a part of our ongoing research into the design of radiopharmaceuticals with enhanced properties for imaging kidney function, we have been exploring the chemistry of $[Re^{V}O]^{3+}$ complexes with BAT ligands derived from L-cysteine (Chart 2) [L-cysH$_n$; H$_n$ indicates the number of dissociable protons present, i.e. −SH, −CO_2H, −NH_2 (listed in decreasing order of acidity upon complex formation)]. One such complex, ReO(ECH$_3$) (ECH$_3$ = trianionic form of ethylenedi-L-cysteine (LL-ECH$_6$) (Chart 2)), has complicated, difficult to interpret NMR spectra in both D_2O[7,9] and DMSO-d_6.[11] The $[Re^{V}O]^{3+}$ complex

Chart 1

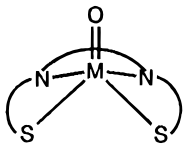

M(V)O(BAT)

[†] Department of Radiology.
[‡] Department of Physics.
[§] Department of Chemistry.
[⊗] Abstract published in *Advance ACS Abstracts,* March 1, 1996.

(1) Van Nerom, C. G.; Bormans, G. M.; De Roo, M. J.; Verbruggen, A. M. *Eur. J. Nucl. Med.* **1993**, *20*, 738.
(2) Verbruggen, A. M.; Nosco, D. L.; Van Nerom, C. G.; Bormans, G. M.; Adriaens, P. J.; De Roo, M. J. *J. Nucl. Med.* **1992**, *33*, 551.
(3) Vallabhajosula, S.; Zimmerman, R. E.; Picard, M.; Stritzke, P.; Mena, I.; Hellman, R. S.; Tikofsky, R. S.; Stabin, M. G.; Morgan, R. A.; Goldsmith, S. J. *J. Nucl. Med.* **1989**, *30*, 599.
(4) Ohmono, Y.; Francesconi, L. C.; Kung, M. P.; Kung, H. F. *J. Med. Chem.* **1992**, *35*, 157.
(5) DiZio, J. P.; Fiaschi, R.; Davison, A.; Jones, A. G.; Katzenellenbogen, J. A. *Bioconjugate Chem.* **1991**, *2*, 353.
(6) Francesconi, L. C.; Graczyk, G.; Wehrli, S.; Shaikh, S. N.; McClinton, D.; Liu, S.; Zubieta, J.; Kung, H. F. *Inorg. Chem.* **1993**, *32*, 3114.
(7) Edwards, D. S.; Cheesman, E. H.; Watson, A. D.; Walovitch, R. In *Technetium and Rhenium in Chemistry and Nuclear Medicine 3*; Nicolini, M., Bandoli, G., Mazzi, U., Eds.; Cortina International: Verona, Italy, 1990; p 433.
(8) O'Neil, J. P.; Wilson, S. R.; Katzenellenbogen, J. A. *Inorg. Chem.* **1994**, *33*, 319.
(9) Marzilli, L. G.; Banaszczyk, M. G.; Hansen, L.; Kuklenyik, Z.; Cini, R.; Taylor, A., Jr. *Inorg. Chem.* **1994**, *33*, 4850.
(10) Jackson, T. W.; Kojima, M.; Lambrecht, R. M. *Aust. J. Chem.* **1993**, *46*, 1093.
(11) Marzilli, L. G.; Hansen, L.; Kuklenyik, Z.; Cini, R.; Banaszczyk, M. G.; Taylor, A., Jr. In *Technetium and Rhenium in Chemistry and Nuclear Medicine 4*; Nicolini, M., Bandoli, G., Mazzi, U., Eds.; SGEditoriali: Padova, Italy, 1995; p 27.

0020-1669/96/1335-1958$12.00/0

Chart 2

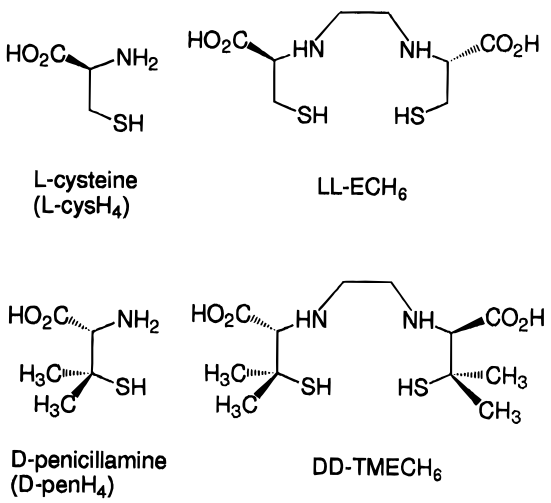

derived from L-cysH$_4$ provided a model system with a simple ^{1}H NMR spectrum since the system lacked the coupled four-spin system of the ethylene bridge in ReO(LL-ECH$_3$). However, the ^{1}H NMR spectrum of both types of compounds was still difficult to analyze due to the coupled three-spin $H_\alpha/H_{\beta'\beta''}$ system of L-cys. The $[Re^{V}O]^{3+}$ complex with D-penicillamine (D-penH$_4$) and its BAT derivative, [ReO(DD-TMECH$_3$)] (DD-TMECH$_3$ = trianionic form of tetramethylethylenedi-D-cysteine (DD-TMECH$_6$) (Chart 2)), provided more useful NMR spectra for interpretation because D-pen has no H_β's. In neutral D_2O, ReO(D-penH$_3$)(D-penH$_2$) (**1**) has the simplest ^{1}H NMR spectrum in this group, consisting of two sets of signals, each with one CH and two CH$_3$ pen signals. Unlike $[M^{V}O]^{3+}$ (M = ^{99}Tc, Re) complexes derived from LL-ECH$_6$ and DD-TMECH$_6$,[7,9] MO(D-penH$_3$)(D-penH$_2$) has a ^{1}H spectrum with sharp signals in D_2O[12] near physiological pH and only one species present in DMSO-d_6.[13]

Since understanding the pH dependence of NMR spectra is crucial in interpreting the behavior of MO(BAT) complexes in solution,[9] we examined the pH dependence of ReO(D-penH$_3$)(D-penH$_2$) (**1**) in D_2O. Unexpectedly, only *one* set of pen signals was observed at pH >12. The simplified ^{1}H spectrum of **1** was intriguing, given the expected symmetry of the complex and the complexity of the spectra of related BAT complexes at high pH. Therefore, **1** was examined by ^{1}H NMR, resonance Raman, UV−visible, and circular dichroism (CD) spectroscopy at different pH's. On the basis of the results of these studies, we offer an explanation for the simplicity of the high-pH ^{1}H NMR spectrum of **1**. This study has led to a clear understanding of the differences and similarities for ReO(NS)$_2$ and ReO(N$_2$S$_2$) complexes.

Experimental Section

UV−visible (UV−vis) and circular dichroism (CD) titrations were performed in D_2O; the pH (uncorrected) was adjusted with NaOD (2.2 M) and DCl (2.2 M). UV−vis spectra were recorded on Shimadzu 3101 and Varian Cary 3 instruments. CD spectra were recorded on a Jasco 600 spectropolarimeter. The FTIR spectrum was obtained using a Nicolet 510M instrument. Potentiometric titration of **1** was carried out using an Orion digital ionalyzer/501 pH meter and calomel electrode standardized with aqueous standard buffers, (pH 10, 7, 4). **1** (0.995 g, 2.0 mmol) was dissolved in a standardized NaOH solution (0.5022 N, 25 mL). The solution was back-titrated with a standardized HCl solution (0.5027 N). An identical titration without the Re complex was also performed. Elemental analyses were obtained from Atlantic Microlabs, Atlanta, GA.

1D ^{1}H NMR Spectroscopy in D_2O and CD_3OD. Spectra were recorded in D_2O, 75% CD_3OD/D_2O, or CD_3OD on a Nicolet 360 or a GE 500 NMR spectrometer and processed with FELIX (Hare Research, Inc.) or MacNMR 5.1. Chemical shifts (ppm) were referenced to TSP (3-(trimethylsilyl)propionic-2,2,3,3-d_4 acid, sodium salt). The pH (uncorrected) was adjusted with NaOD (2.2 M) or DCl (2.2 M) and NaOD/75% CD_3OD (2.2 M) and measured with a long-stem pH electrode. $NaOCD_3$ (4 M) was prepared by addition of Na to CD_3OD.

2D NMR Spectroscopy in DMSO-d_6. ^{1}H−^{13}C heteronuclear multiple-quantum correlation experiments (HMQC/HMBC) were performed on a GE 500 NMR spectrometer at 27 °C using 50 mM sample concentration. Totals of 1024 t_2 and 128 t_1 points were collected, with 94 scans for the HMQC and 288 scans for the HMBC experiment. All 2D data were processed with FELIX (Hare Research, Inc.), zero-filled to 1024 points in the t_1 dimension, and Fourier-transformed after using a 0° shifted sine bell window function in both dimensions. The ^{1}H and ^{13}C signals from DMSO-d_6 at 2.49 and 39.50 ppm, respectively, were used as references.

Resonance Raman Spectroscopy. Resonance Raman measurements were made with samples in melting point capillaries with excitations at 406.7 nm from a krypton ion laser (Coherent Innova 100). Power at the samples was kept below 20 mW. Raman signals were collected via 90° geometry by a triple monochromator (Spex Model 1877 Triplemate) with a photodiode array detector consisting of a Model IRY-1024 detector and a Model ST-120 controller from Princeton Instruments that was interfaced to an IBM-AT microcomputer. Calibrations were performed for each measurement by using known Raman lines of toluene. Peak positions were accurate to within ±1−2 cm^{-1} between runs. Typical resolution was 6−8 cm^{-1}. For all samples, no changes (both spectral features and intensities) were observed in the Raman spectra as a function of exposure time to the laser. Concentrations of Re complex were ∼40 mM for titrations in D_2O; the pH (uncorrected) was adjusted with NaOD (2.2 M) and DCl (2.2 M). For samples in dry MeOH, concentrations of Re complex were ∼20 mM. MeOH was dried with Na and distilled under N_2. NaOMe solutions (4 M) were prepared by adding Na to dry MeOH. Re−^{18}O frequencies for **1** were obtained by dissolving the complex in 80% $^{18}OH_2$. The pH was adjusted with NaOH/^{18}OH (1 mM) until the Re−^{16}O band frequency matched that found in the D_2O spectra at the desired pH. The rate of ^{18}O to ^{16}O exchange in **1** was also monitored by resonance Raman spectroscopy. An ^{18}O sample was prepared by dissolving **1** in D_2O with 1 equiv of NaH_2PO_4 (0.01 mM, 1 mL) and adjusting the pH to 7.0. The solution was lyophilized, and the residue was dissolved in $^{18}OH_2$ (93.7%, 25 μL) and allowed to exchange overnight. The sample was lyophilized, and a portion (1.5 mg) was redissolved in $^{16}OH_2$ buffered with NaH_2PO_4 (1.2 mM, 75 μL). The first resonance Raman measurement was obtained at 42 s, followed by a measurement every 15 s until the exchange was complete. The final pH of the sample was 6.8.

Syntheses. ReO(D-penH$_3$)(D-penH$_2$) (1). The preparation of **1** was similar to a literature procedure.[12] Ammonium perrhenate (134 mg, 0.5 mmol) and D-penH$_4$ (200 mg, 1.3 mmol) were dissolved in 1 N HCl (10 mL), and the solution was cooled to 5 °C. A solution of $SnCl_2 \cdot 2H_2O$ (125 mg, 0.6 mmol) in 1 N HCl (1 mL) was added dropwise over 10 min. Stirring of this reaction solution was continued for 10 min at 5 °C and an additional 10 min at room temperature. The dark precipitate that formed was collected and redissolved in H_2O (3 mL) by adding 1 N KOH (pH 5−6). The solution was filtered and the filtrate acidified with 1 N HCl (pH 1−2), cooled to 5 °C, and left to stand overnight. Violet microcrystals were collected and vacuum-dried. Yield: 0.16 g (64%). Anal. Calcd for $C_{10}H_{19}N_2O_5ReS_2$: C, 24.14; H, 3.85; N, 5.63. Found: C, 24.09; H, 3.88; N, 5.59. FTIR in KBr: 972 cm^{-1} [Re═O].

Results

NMR. Although our goal is to understand the solution properties of **1** in aqueous solution, the NMR signal assignments are best done in DMSO-d_6. The signal assignments in aqueous

(12) Johnson, D. L.; Fritzberg, A. R.; Hawkins, B. L.; Kasina, S.; Eshima, D. *Inorg. Chem.* **1984**, *23*, 4204.
(13) Franklin, K. J.; Howard-Lock, H. E.; Lock, C. J. L. *Inorg. Chem.* **1982**, *21*, 1941.

Table 1. ^{1}H and ^{13}C NMR Chemical Shift Assignments (ppm) for ReO(D-penH$_3$)(D-penH$_2$) (**1**)

Solvent	H_α		Me'		Me"		NH		H_{COO}
	syn-	*anti*-	*syn*-	*anti*-	*syn*-	*anti*-	*syn*-	*anti*-	
DMSO-d_6	2.95	3.59	1.87	1.61	1.27	1.44	6.57[a]	5.74[a]	13.44
							7.58[b]	7.69[b]	
D_2O, pH 7.6	3.12	4.07	2.07	1.83	1.28	1.66			
D_2O, pH 12.2	3.19		1.83		1.16				
CD_3OD	3.26	3.82	2.01	1.73	1.31	1.62			
	C_α		C_β		$C_{Me'}$		$C_{Me"}$		CO_2
	syn-	*anti*-	*syn*-	*anti*-	*syn*-	*anti*-	*syn*-	*anti*-	
DMSO-d_6	69.90	72.86	59.99	55.88	29.51	30.31	24.27	28.32	171.21[a]
									173.76[b]

[a] *syn*-, [b] *anti*-.

Chart 3

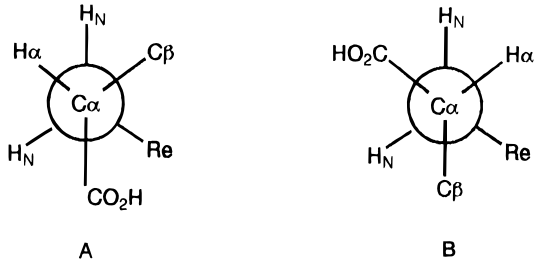

solution were obtained by following the signals in DMSO-d_6/D_2O mixtures. The ^{1}H and ^{13}C spectra of **1** in DMSO-d_6 (Table 1) consisted of two sets of pen signals and are similar to the spectra reported for ^{99}TcO(D-penH$_3$)(D-penH$_2$) in DMSO-d_6.[13] A complete assignment of the NMR spectrum of ^{99}TcO(D-penH$_3$)(D-penH$_2$) was not reported; however, the two sets of pen signals were stated to be consistent with its solid-state structure.[13] In the solid-state structure of ^{99}TcO(D-penH$_3$)(D-penH$_2$), the two D-pen ligands coordinate in the basal plane and form a *cis* isomer; thus, the two CO_2 groups are oriented to opposite sides of the N_2S_2 coordination plane. The CO_2 *anti* to the oxo ligand is deprotonated and coordinated (*anti*-CO_2-bound). The CO_2 *syn* to the oxo ligand is protonated and not coordinated (*syn*-CO_2H).

In the downfield region of the 1D ^{1}H spectrum of **1**, there are four NH signals but only one CO_2H signal (which integrates to one proton). Therefore, as in the solid-state structure of ^{99}TcO(D-penH$_3$)(D-penH$_2$), one CO_2 group is deprotonated. The CH, CO_2, CMe_2, and NH ^{1}H/^{13}C signals belonging to the same pen residue were correlated through $^1J_{HC}$ coupling peaks in the HMQC spectrum and $^2J_{HC}$ and $^3J_{HC}$ coupling peaks in the HMBC spectrum. The assignments of the two sets of pen signals to *anti* and *syn* ligands were based on the following conformational considerations.

The *syn* and the *anti* coordinated ligands each could be in one of two conformations (**A** and **B** in Chart 3). Only conformation **B** has a *trans* $H_\alpha-C_\alpha-N-H$ torsion angle which causes strong $H_\alpha-NH$ coupling. In the downfield region of the 1D ^{1}H spectrum of **1** in DMSO-d_6 (Figure 1), the one triplet NH signal indicates strong $H_\alpha-NH$ coupling, while the three doublet NH signals indicate weak $H_\alpha-NH$ couplings. Therefore, only one D-pen ligand is in conformation **B**.

The NMR data are consistent with two models: model 1, with the *anti* ligand in conformation **A** and the *syn* ligand in conformation **B**, and model 2, with the *anti* and *syn* ligands in conformations **B** and **A**, respectively. In model 2, the *syn*-CO_2 group either has unfavorable contacts with the oxo ligand or binds in the basal plane, forcing the N of the same ligand into the axial position *trans* to the oxo ligand. Although an NOS_2 donor set in the basal plane is unusual, it does occur in the solid-state structure of *syn*-ReO(DL-ECH$_3$)·3H$_2$O.[14] However, *syn*-ReO(DL-ECH$_3$) also has an unusual Re=O resonance Raman frequency in D_2O (952 cm^{-1}). The Re=O resonance Raman frequency in D_2O of **1** (969 cm^{-1}) (see below) is similar to those reported for complexes with an N_2S_2 donor set in the basal plane and the *anti*-CO_2 bound *trans* to the oxo ligand, i.e. ReO(DD-TMECH$_3$) (974 cm^{-1}) and ReO(LL-ECH$_3$) (976 cm^{-1}).[15] Thus, we rule out model 2 and strongly favor model 1, which is consistent with the structure of ^{99}Tc(D-penH$_3$)(D-penH$_2$).[13]

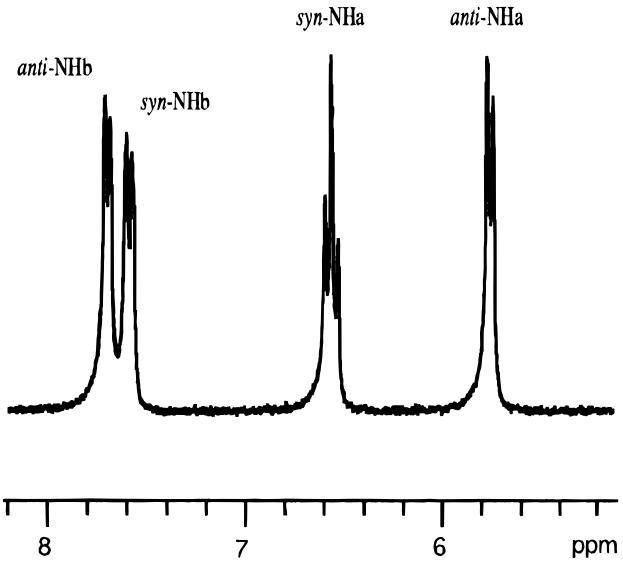

Figure 1. Downfield region of the ^{1}H NMR spectrum of ReO(D-penH$_3$)(D-penH$_2$) (**1**) in DMSO-d_6.

Thus, for **1**, the triplet NH signal and the set of the ^{1}H and ^{13}C signals correlated to it by HMQC and HMBC cross-peaks were assigned to the *syn* ligand, and the other set of signals to the *anti* ligand. The signal assignments for the Me′/Me″ and

(14) Hansen, L.; Lipowska, M.; Taylor, A., Jr.; Marzilli, L. G. *Inorg. Chem.* **1995**, *34*, 3579.
(15) Hansen, L.; Xu, X.; Yue, K. T.; Lipowska, M.; Taylor, A., Jr.; Marzilli, L. G. Manuscript in preparation.

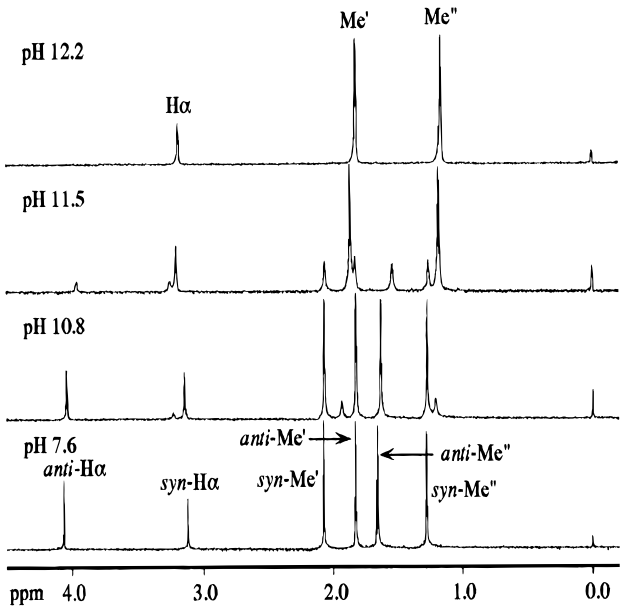

Figure 2. ^{1}H NMR spectra of ReO(D-penH$_3$)(D-penH$_2$) (**1**) in D_2O at various pH values (uncorrected).

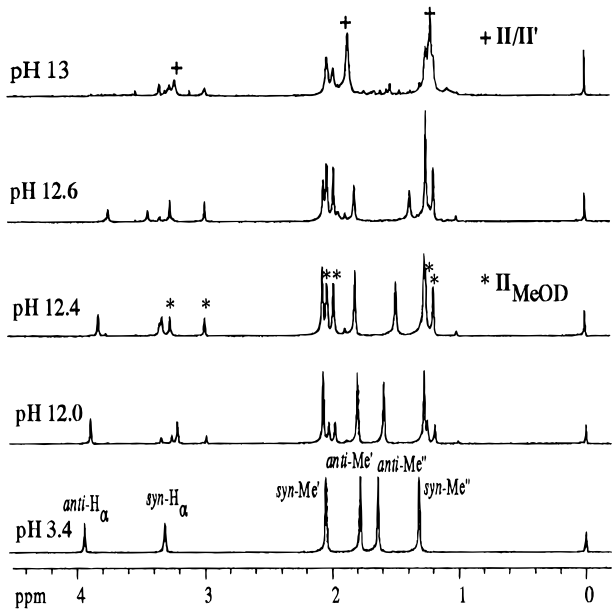

Figure 3. ^{1}H NMR spectra of ReO(D-penH$_3$)(D-penH$_2$) (**1**) in 75% CD_3OD/D_2O at various measured pH values (uncorrected) (+, **II/II′**; *, **II**$_{MeOD}$).

Chart 4

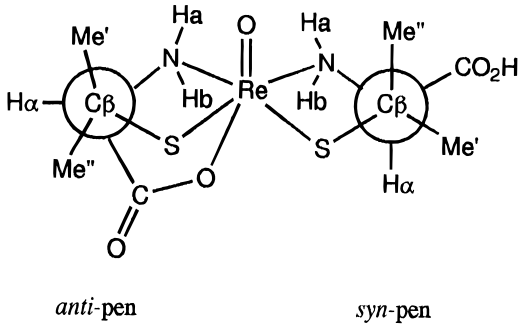

syn/anti-NH geminal pairs in Table 1 are based on comparison of the expected ^3J couplings for model 1 (Chart 4) with the couplings in the 1D ^{1}H spectra and with the relative intensities of the cross-peaks in the HMBC spectra. Because of the *trans* torsion angles in model 1, relatively strong ^3J couplings are expected between *syn*-H$_α$ and *syn*-H$_a$ of **1**. Similarly, relatively strong HMBC cross-peaks are expected between *syn*-H$_α$ and *syn*-Me" and between *anti*-CO_2 and *anti*-H$_a$.

The ^{1}H NMR spectrum of **1** in D_2O (Table 1) was assigned by the mixed-solvent experiments. **1** is insoluble in its neutral form, and in the starting 100% D_2O solutions studied by NMR the *syn*-CO_2 group is deprotonated and the complex is monoanionic (form **I**). The spectrum of **1** at pH 7.6 consisted of two sets of pen signals (Figure 2). However, at pH 10.8 a new single set of pen signals emerged. With increasing pH, the original pen signals decreased in intensity and both H$_α$ and the *anti*-Me" signals shifted. The new set of signals increased in intensity, and each signal shifted upfield. At pH 12.2, only the new single set of pen signals was observed.

These results suggest that for **1** the pH 7−9 form (**I**) converts to a mixture of a related species (**I′**) and a form with different characteristics (**II**). A third form (**II′**), related to **II**, emerges at higher pH.

In 75% CD_3OD/D_2O (measured pH 3.5), the ^{1}H NMR spectrum of ReO(D-penH$_3$)(D-penH$_2$) (**1**) (Figure 3) also consisted of two sets of pen signals (**I**). At a measured pH value of 12.0, a new species with two sets of pen signals emerged (**II**$_{MeOD}$). With additional base, the original signals shifted and decreased in intensity while those of **II**$_{MeOD}$ increased in intensity. The shift indicates that **I′** is formed. As more NaOD was added, an additional species appeared; this species had one set of pen signals similar to those of **II/II′** in the high-pH D_2O spectrum of **1**; the signals of **II/II′** increased in intensity and those of **II**$_{MeOD}$ decreased in intensity. In 50% CD_3OD/D_2O, **II**$_{MeOD}$ and **II/II′** emerged near a measured pH value of 11.4. As more NaOD was added, the signals of **I/I′** declined in intensity and shifted. The signals of **II**$_{MeOD}$ and **II/II′** increased in intensity, but only those of **II/II′** shifted. Thus **II**$_{MeOD}$ behaved differently from **II**.

1 was soluble in dry CD_3OD with 1 equiv of $NaOCD_3$ added. The ^{1}H NMR spectrum of the solution was similar to the pH 7−9 D_2O and CD_3OD/D_2O spectra of **1.** One species with two sets of pen signals was present, indicating that the added base was consumed by deprotonation of the *syn*-CO_2H group. Addition of >1 equiv of $NaOCD_3$ produced a new species with two sets of pen signals (**II**$_{MeOD}$) and shifts in the original signals consistent with a **I** to **I′** fast equilibration. As the amount of $NaOCD_3$ added was increased, the signals of **II**$_{MeOD}$ increased in intensity (Figure 4) but did not shift (Figure 5); the **I/I′** signals decreased in intensity (Figure 4) and continued to shift (Figure 5). However, with $NaOCD_3$:**1** molar ratios of ∼5 and greater, the **I/I′** signals did not shift further and the intensity ratio of the **I/I′** to **II**$_{MeOD}$ signals remained constant. **II′** was not observed.

In both 75% CD_3OD/D_2O and dry CD_3OD, a minor unidentified species (with one set of pen signals) was formed upon addition of base. The signals were most apparent in the CD_3OD spectra. The intensities of the signals did not change significantly as more base was added, and the chemical shifts of the signals did not correspond to those of free pen under similar conditions. Although this minor species has one set of pen signals similar to those of **II**, both forms were present in 75% CD_3OD/D_2O and the chemical shifts of their signals were distinctly different.

Resonance Raman. Strong Re═O resonance Raman (high-frequency) bands were observed for **1** (969 cm^{-1}) in acidic, neutral, and moderately basic aqueous solutions (Table 2). A new broader (mid-frequency) band at 930 cm^{-1} appeared near pH 11. The new band increased in intensity while the high-frequency band decreased in intensity with increasing pH. A

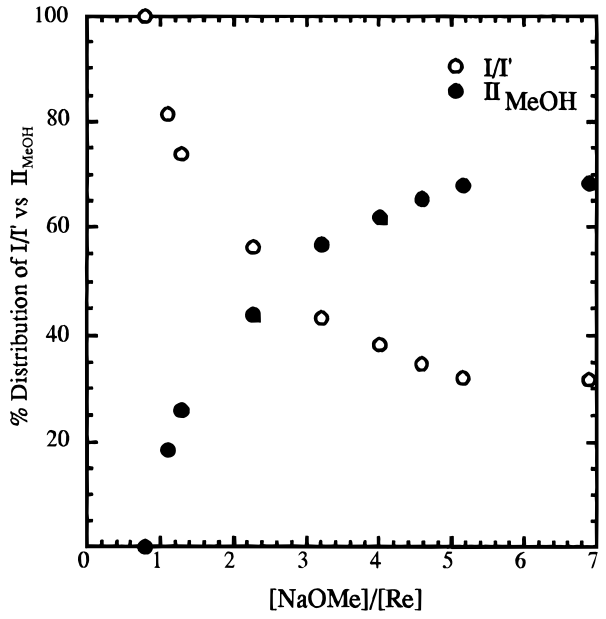

Figure 4. Percent distribution of **I/I′** and $\mathbf{II}_{MeOH}$ in the ^{1}H NMR spectrum of ReO(D-penH$_3$)(D-penH$_2$) (**1**) in CD$_3$OD with addition of NaOCD$_3$.

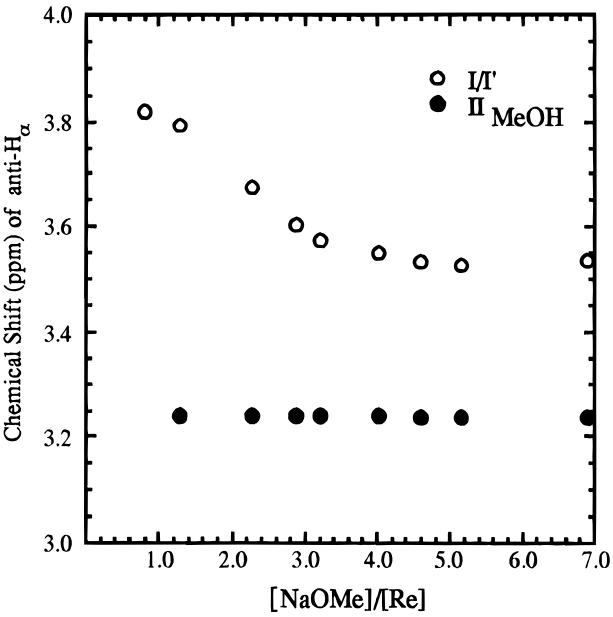

Figure 5. Chemical shifts of the H$_\alpha$ protons of **I/I′** and $\mathbf{II}_{MeOH}$ in the ^{1}H NMR spectrum of ReO(D-penH$_3$)(D-penH$_2$) (**1**) in CD$_3$OD with addition of NaOCD$_3$.

Table 2. Resonance Raman Re═O Band Frequencies ($\Delta\nu$, cm^{-1}) for ReO(D-penH$_3$)(D-penH$_2$) and Re^{18}O(D-penH$_3$)(D-penH$_2$)

complex	high $\Delta\nu$	mid $\Delta\nu$	low $\Delta\nu$
ReO(D-penH$_3$)(D-penH$_2$)	969	930	846
Re^{18}O(D-penH$_3$)(D-penH$_2$)	922	882	799

weak low-frequency band (846 cm^{-1}) emerged at approximately 1 pH unit above the pH at which the mid-frequency band first appeared and increased in intensity with increasing pH. At pH 12.9, the low-frequency band predominated even though the high- and mid-frequency bands were still distinguishable. The changes observed in the Raman spectra at high pH values are shown in Figure 6. For **1**, the high-frequency Raman band and the low-pH form observed by NMR (**I**) were observed over the same pH range. The mid-frequency Raman band emerged in the same pH range that the signals of **I/I′** shifted, and the high-pH form observed by NMR (**II**) emerged. As the low-frequency

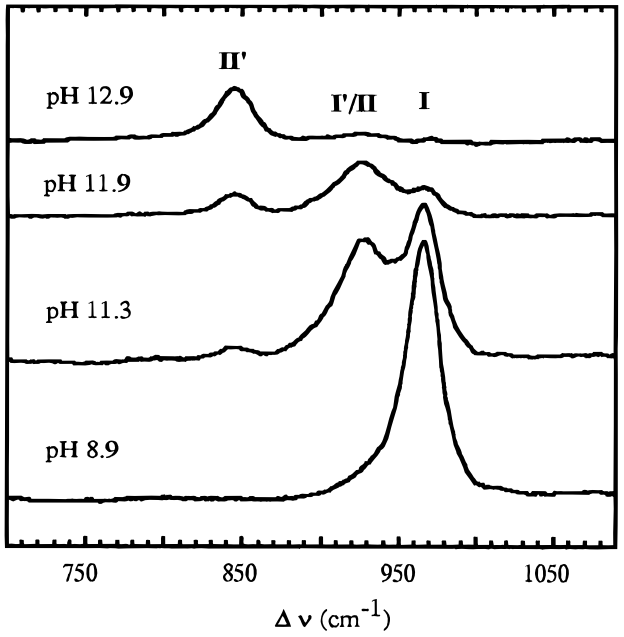

Figure 6. Resonance Raman spectra of ReO(D-penH$_3$)(D-penH$_2$) (**1**) in D$_2$O at various pH values (uncorrected).

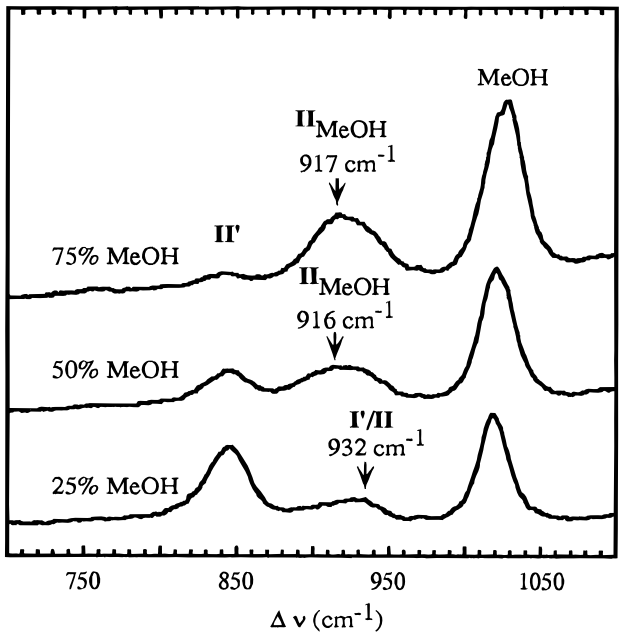

Figure 7. Resonance Raman spectra of ReO(D-penH$_3$)(D-penH$_2$) (**1**) in MeOH/H$_2$O solutions, pH ∼13.

Raman band emerged, the NMR signals of the high-pH form (**II/II′**) shifted upfield, consistent with the shifting equilibria.

In MeOH/H$_2$O mixtures, the Re═O band of **1** was observed at 966−968 cm^{-1}. However, near pH 12 this band was replaced by a band at 930−933 cm^{-1} which remained relatively strong until the pH approached 13. Under these extreme conditions, the intensity of the band at 930−933 cm^{-1} decreased. In 75% MeOH and 50% MeOH mixtures, the declining band revealed a weak band at 916−917 cm^{-1}. In 25% MeOH, a similar band was not observed. In all three MeOH/H$_2$O mixtures, a low-frequency band (842−847 cm^{-1}) was generated but its intensity was inversely related to the MeOH concentration; i.e., the band was weak in 75% MeOH and strong in 25% MeOH (Figure 7).

In dry MeOH, addition of dry NaOMe (3 equiv) shifted the Re═O band of **1** from 972 to 933 cm^{-1}; however, the new band had a low-frequency shoulder (Figure 8). The shape of the new band remained relatively constant with up to ∼9 equiv of

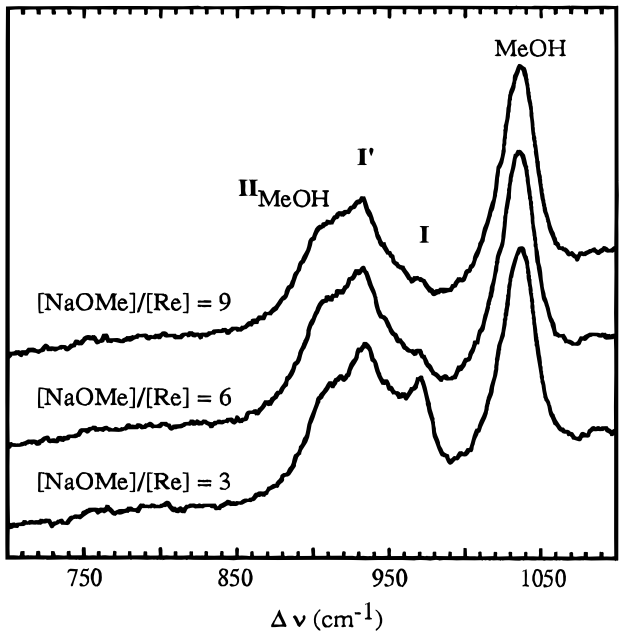

Figure 8. Resonance Raman spectra of $ReO(D\text{-}penH_3)(D\text{-}penH_2)$ (**1**) in MeOH with addition of NaOMe.

Table 3. UV−Visible and Circular Dichroism Maxima for $ReO(D\text{-}penH_3)(D\text{-}penH_2)$ (**1**)

UV−Visible					
pH	λ_{max} (nm)	ϵ ($M^{-1}\,cm^{-1}$)	pH	λ_{max} (nm)	ϵ ($M^{-1}\,cm^{-1}$)
7	342	4.1×10^3	12	290	3.3×10^3
	504	93		420	99
Circular Dichroism					
pH	λ_{max} (nm)	10^{-4} ($\Delta\epsilon$) ($M^{-1}\,cm^{-1}$)	pH	λ_{max} (nm)	10^{-4} ($\Delta\epsilon$) ($M^{-1}\,cm^{-1}$)
7	496	−4.2	12	426	−1.0
	341	7.5		291	3.0
	284	−1.0			

NaOMe added, consistent with an equilibrium mixture of **I′** and **II**. The low-frequency band observed in D_2O (846 cm^{-1}) was absent.

The rate of ^{18}O (922 cm^{-1}) to ^{16}O (969 cm^{-1}) exchange was monitored from the rate of disappearance of the Re═^{18}O band. Isotopic exchange of the oxo ligand in **1** was rapid ($t_{1/2}$ ~75 s) when the complex was dissolved in $^{18}OH_2$ at a pH value as low as 6.8. Each of the three pH-dependent resonance Raman bands was shifted to lower frequency by 47−48 cm^{-1} on ^{18}O labeling (Table 2).

UV−Visible Spectroscopy and Circular Dichroism (CD). The UV−vis and CD spectra of **1** in D_2O (Table 3) showed no appreciable change over a wide pH range. However, at high pH, the absorption spectra exhibited changes in two phases. First, the intensity of the UV band (342 nm) decreased sharply from pH 10.4 to 11.0 (Figure 9). The intensity of the visible band also decreased in this pH range, but the change was small. At pH 11.0, two maxima (342 and 290 nm) were present in the UV region. A second phase was observed as the pH was raised above 11.0. The new UV band (290 nm) increased in intensity as the band at 342 nm continued to decline; there was no isosbestic point. Concurrently, the intensity of the visible band decreased sharply (Figure 10). A visible band at 420 nm was not noticeable until pH 12.4 due to the overlapping absorption from the tail of a band in the UV region at lower pH values.

The first phase changes occurred in the same pH range in which the NMR signals of **I**/**I′** were shifting and declining and

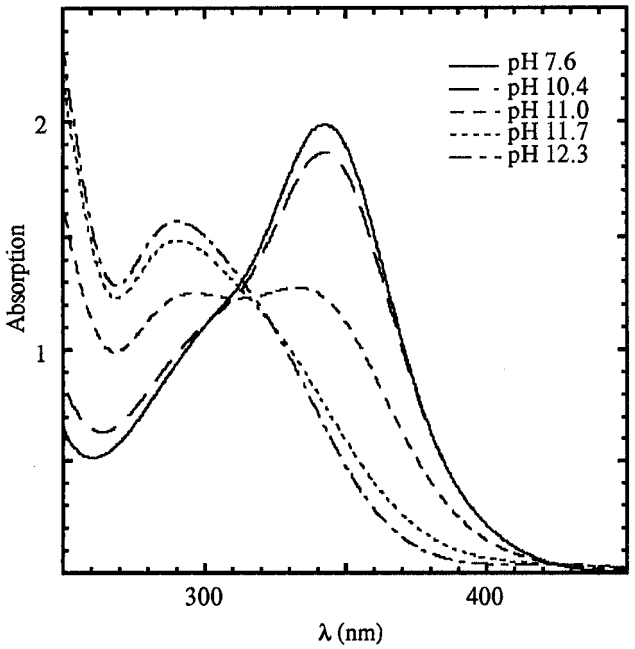

Figure 9. Ultraviolet spectra of $ReO(D\text{-}penH_3)(D\text{-}penH_2)$ (**1**) (4.8×10^{-4} M) in D_2O at various pH values (uncorrected).

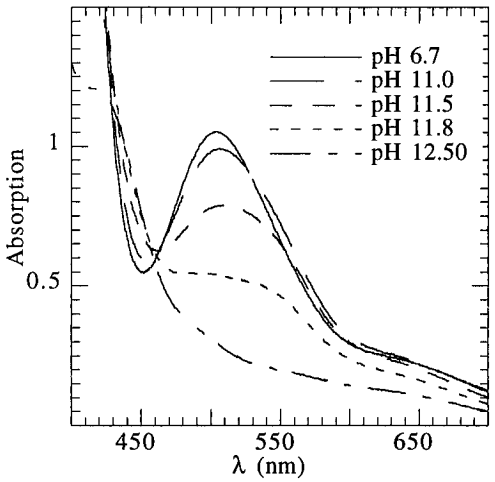

Figure 10. Visible spectra of $ReO(D\text{-}penH_3)(D\text{-}penH_2)$ (**1**) (1.1×10^{-2} M) in D_2O at various pH values (uncorrected).

those of form **II** were emerging. Also, the mid-frequency band appeared in the Raman spectrum. In the second-phase pH range, the low-frequency band emerged in the resonance Raman spectrum. These phases were not so evident in the CD spectra, where the transitions occurred smoothly (Figure 11); however, an isodichroic point was absent in the visible region. The absence of isosbestic points in the UV−vis and an isodichroic point in the visible region of the CD spectra suggest that the low-pH form converts to more than one new form at high pH. The apparent isodichroic point in the UV region of the CD spectra indicates that **I**, **I′**, and **II** have similar spectra in this region.

pH Titrations. Solutions containing 12.6 mmol of NaOH were titrated with HCl. The titration curves for **1** (Re curve) and an identical titration without the Re complex (control curve) are shown in Figure 12. The Re curve shows an inflection between pH 11 and 12 and is displaced along the ordinate with respect to the control curve. The displacement reflects the difference in the amount of HCl required to achieve a particular pH value in the presence and absence of **1**. The ratio of the difference in the amount of HCl (mmol) added/mmol of Re is

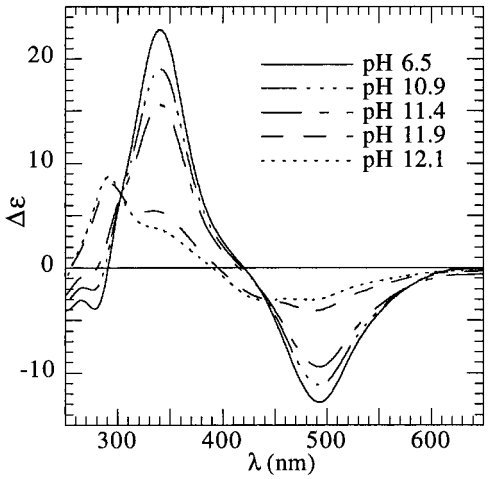

Figure 11. CD spectra of ReO(D-penH$_3$)(D-penH$_2$) (**1**) (2.3×10^{-4} M) in D_2O at various pH values (uncorrected).

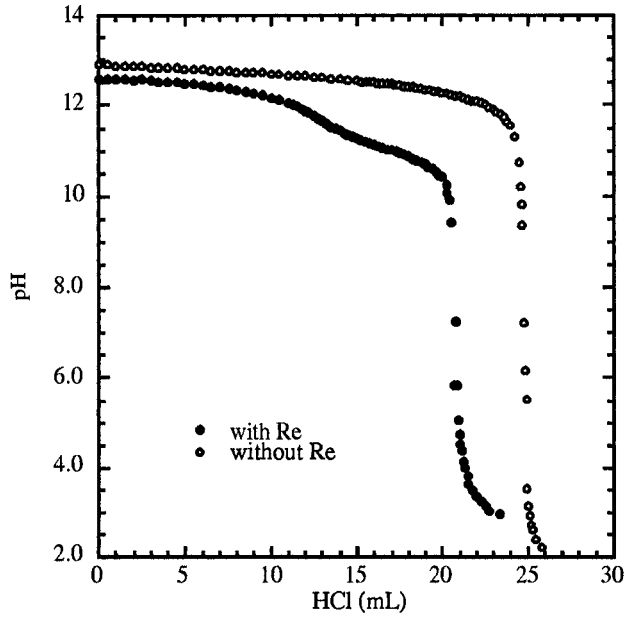

Figure 12. Plot of pH vs HCl (mL) added in the titration of ReO(D-penH$_3$)(D-penH$_2$) (**1**) and in a control titration (without complex added).

plotted vs pH in Figure 13. The data show that roughly 3 equiv of H^+ is consumed by **1**. Two equivalents is titrated above pH 10. At pH ~12, where the amount of **I′/II** and the mid-frequency Raman band are maximal, approximately half of these 2 equiv of base was titrated. The third equivalent (consumed at pH ~3) protonates the *syn*-carboxyl group. Below pH 3.0, **1** precipitated and the Re titration was discontinued.

Discussion

As outlined in the Introduction, our initial expectation in investigating ReO(D-penH$_3$)(D-penH$_2$) (**1**) was that it would serve as a simple model system for interpreting the complicated spectral behavior of the MO(BAT) (M = Re, Tc) derivatives. Previous studies determined that ^{99}TcO(D-penH$_3$)(D-penH$_2$)[13] and ReO(LL-ECH$_3$)[9] share a common coordination environment in the solid state: six-coordination with a deprotonated *anti*-CO_2^- coordinated to the metal *trans* to the oxo ligand; *cis*-coordination of the N (and S) donor atoms of the two D-pen ligands in ^{99}TcO(D-penH$_3$)(D-penH$_2$). **1** and related MO(BAT) complexes precipitate from H_2O when the pH is lowered to values below their respective pK_{a1} values (corresponding to protonation of the *syn*-CO_2); these complexes have similar Re═O stretching frequencies in their neutral solid-state forms.

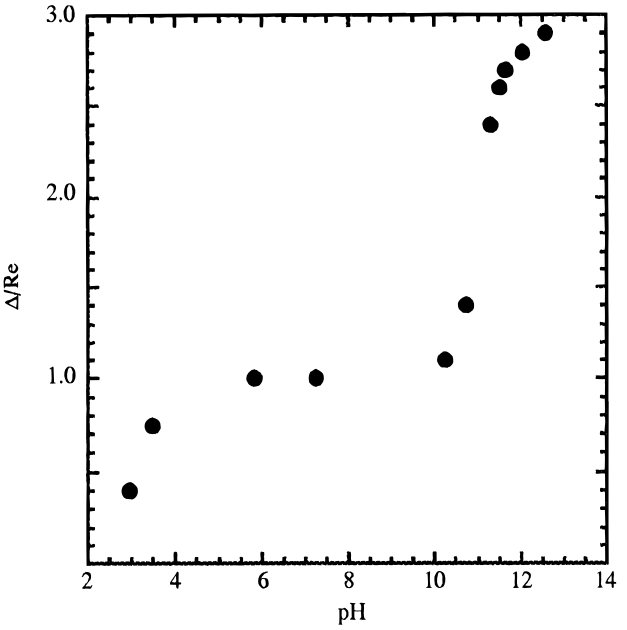

Figure 13. Plot of Δ/Re (difference in the amount of HCl (mmol) titrated in the control titration and with ReO(D-penH$_3$)(D-penH$_2$) (**1**)/mmol of **1**) vs pH.

As is evident from the results presented above, **1** did not prove to have the desired quality of simplicity needed in a model system. However, its unusual characteristics appeared to be worth understanding, in the hope that further insight into the properties of ReO(N_2S_2) complexes would emerge. In the meantime, we utilized the related D-pen analog for LL-EC, DD-TMEC, to elucidate the very complicated properties of [MO(LL-ECH$_2$)]$^-$ derivatives near neutral pH. We found that the singly *syn*-carboxyl-deprotonated [ReO(DD-TMECH$_2$)]$^-$ species became doubly deprotonated near neutral pH, but the process was not simple; the "pK_{a2}" process involved *anti*-NH deprotonation coupled to *anti*-CO_2^- deligation.[9] The overall process occurs in the intermediate time domain on the NMR time scale and produces very broad NMR signals near pH 7. Analysis of the NMR signals leaves little doubt concerning the ligation state of the DD-TMEC ligand, which changes from a denticity of 5 below pH 6 to 4 above pH 8. A mixture exists at pH 7 for the EC-type complexes. An X-ray structural analysis of the fully deprotonated [ReO(LL-EC)]$^{3-}$ complex shows it is five-coordinate,[9] and it appears likely that this form is five-coordinate in solution. However, the doubly deprotonated [ReO(DD-TMECH)]$^{2-}$ and [ReO(LL-ECH)]$^{2-}$ could be either five- or six-coordinate, with solvent bound in the axial position.

Our results on the effects of base on ReO(*anti*-D-penH$_3$-*N,S,O*)(*syn*-D-penH$_2$-*N,S*) do shed light on the properties of EC-type complexes (see Conclusions). In Scheme 1 we present our interpretation of the results. First, we will discuss D-pen ligation in **I/I′** and **II/II′**, and then we will discuss the effects of base in more detail.

The NMR spectrum in DMSO-d_6 clearly indicates the carboxyl-ligated form is present, and the smooth shifts in signals between solvents demonstrate that this form exists also in water and methanol. On the NMR time scale, the **I** ⇔ **I′** and the **II** ⇔ **II′** exchanges are fast but the **I/I′** ⇔ **II/II′** exchange is slow. These results strongly suggest that the fast process that relates **I** to **I′** and **II** to **II′** is protonation/deprotonation in D_2O. The evidence to be discussed below strongly indicates that the slow process between these pairs is ligation/deligation of the D-pen carboxyl group.

In the D_2O ^{1}H NMR spectra of **1** (Figure 2), some signals of form **I** shifted as the second proton equivalent was titrated

Scheme 1

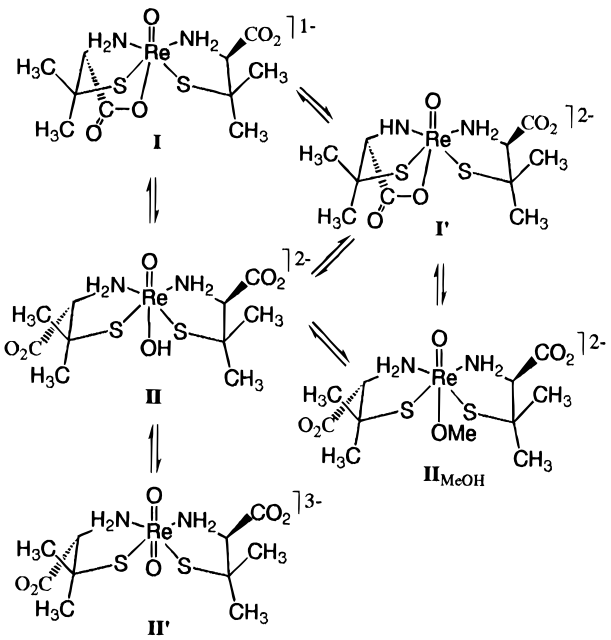

(Figures 12 and 13). Simultaneously, the signals of the high-pH form (**II**) emerged. These results indicate that deprotonation to form **I′** and the formation of **II** occur in parallel, each process consuming a proportionate amount of the 1 equiv of base. If **II** were simply deprotonated, it would be in fast exchange with **I′**. The only reasonable interpretation is that **II** has deligated carboxyls and hydroxo coordinated *trans* to the oxo group. Such a species allows us to explain our spectroscopic observations and ^{18}O exchange data.

The high-frequency Re═O band of **I** decreased and a broad mid-frequency band appeared as **I′** and **II** formed (Figure 6). The formation of more than one species with similar Re═O bands was probably responsible for the broadness of the mid-frequency band. At pH ∼11, the intensity of the UV band decreased (perhaps a result of deprotonation), but the visible band remained relatively unchanged (Figures 9 and 10). The CO_2-bound (**I**/**I′**) and hydroxo-bound (**II**) species may have similar visible spectra. At higher pH, the visible spectrum changed significantly but there were less drastic changes in the UV spectrum. Again, this is consistent with multiple species.

Rapid proton exchange from hydroxo to oxo in form **II** will equilibrate the oxo and hydroxo ligands above and below the N_2S_2 plane. The effect of the exchange is to create a time-averaged C_2 axis in the N_2S_2 plane, bisecting the two ligands. This explanation requires that oxo group exchange be particularly favorable since only one set of pen signals for **II** was observed at the lowest pH at which **II** was detectable. ^{18}O exchange was too fast for us to measure above pH 7. At pH 6.8, the observed half-life for ^{18}O exchange of ∼1 min gives a k_{obs} of $\sim 10^{-2}$ s^{-1}. Estimating that half the complex exists as [ReO(*anti*-D-penH$_2$-*N*,*S*)(*syn*-D-penH$_2$-*N*,*S*)OH]$^{2-}$ (form **II**) at pH 11.8, then the equilibrium constant for the formation of **II** from **I** and OH$^-$ is $\sim 10^2$ M^{-1}. At pH 6.8, only 1/10^5 of the Re is in form **II**. Therefore, the pseudo-first-order exchange rate is $\sim 10^3$ s^{-1}. This gives a very high second-order rate constant of 10^{10} M^{-1} s^{-1}, if OH$^-$ catalyzes the proton transfer from the coordinated OH to the oxo group. Although the estimate is crude, it suggests that the oxo group exchange process is extremely facile for form **II**, a conclusion consistent with the NMR data.

As the pH increased, in the high-pH range >11.5 in D_2O, the third equivalent of OH$^-$ was taken up (Figures 12 and 13), the ^1H NMR signals of **II** shifted upfield (Figure 2), and the low-frequency Re═O Raman band emerged (Figure 6). If **II** is a six-coordinate hydroxo/oxo complex, it is unlikely that a second hydroxo ligand can add, since the addition would increase the coordination number. Thus, these changes indicate that the next equivalent of base deprotonates **II** at NH or the axial OH; either deprotonation process is consistent with the fast **II**/**II′** exchange.

To gain further insight into the nature of **II** and **II′**, we carried out experiments in CD_3OD and CD_3OD/D_2O mixtures. The methoxo ligand cannot deprotonate; creation of the pseudo-C_2 axis by the above mechanism is not possible. In 50% CD_3OD (measured pH ≥11.4), 75% CD_3OD (measured pH ≥12) (Figure 3), and dry CD_3OD (with >1 equiv of $NaOCD_3$), the signals of **I** shifted (**I**/**I′** fast equilibration) as those of **II**$_{MeOD}$ emerged. **II**$_{MeOD}$ displayed two equal-intensity sets of D-pen NMR signals, as expected for a methoxo-bound species (Scheme 1). In methanol/water mixtures, the **II**/**II′** forms were generated along with **II**$_{MeOD}$ as base was added. Since **II**$_{MeOD}$ and **II**/**II′** coexist in mixed-solvent systems, these species must be six-coordinate with bound solvent. In 50% D_2O, the signals of species derived from D_2O (**II**/**II′**) were large and could be observed over a measured pH range wide enough to allow detection of shift changes. These shifts were consistent with an equilibrium mixture shifting from **II** to **II′** with added base. The NMR signals of **II**$_{MeOD}$ did not shift with changes in basicity. In 100% methanol the mid-frequency Raman band had a distinct low-frequency shoulder at 916−917 cm^{-1} that did not change as more base was added (up to ∼9 equiv) (Figure 8). The intensity ratio of the ^1H NMR signals of **I**/**I′** and **II**$_{MeOH}$ remained constant after addition of 5 equiv of base (Figure 4). This is consistent with an equilibrium mixture of **I′** and **II**$_{MeOH}$. The independence of the ratio of **I′** to **II**$_{MeOH}$ is in agreement with the conclusions from the D_2O studies that **I′** and **II** are formed from **I** as a mixture and that the formation requires 1 equiv of base. For all solvent systems studied, a band was observed at 930−933 cm^{-1}, consistent with the presence of **I′**. The shoulder at 916−917 cm^{-1} was observed only in methanol solutions, consistent with the presence of a band for **II**$_{MeOH}$.

The Re═O band of **I′** was shifted ∼40 cm^{-1} compared to that of **I** (Table 2); this difference reflects the effect of NH deprotonation. However, the Re═O band of **II′** was shifted ∼80 cm^{-1} compared to that of **II**, a difference twice that expected for NH deprotonation. It is significant that the low-frequency Re═O band characteristic of **II′** was not observed in the absence of water. The results suggest that, instead of NH deprotonation, **II** deprotonates at the coordinated OH site, producing a *trans*-dioxo species (**II′**) (Scheme 1). Deprotonation of a *trans* HO−Re═O system to give a *trans* O═Re═O system explains the large shift (∼80 cm^{-1}) in the frequency of the Re═O band. The frequency of the band of **II′** (846 cm^{-1}) also falls well within the range of metal-oxo stretching frequencies observed for known *trans*-dioxo complexes (768−895 cm^{-1}).[16] We believe that this explanation is more consistent with the results than the alternative possibility that **II′** is a OH-ligated, NH-deprotonated species. This alternative would require that the related species **II** and **II**$_{MeOD}$ had very different NH acidities in the same solvent (50% CD_3OD).

Combined resonance Raman and NMR data in methanol−water mixtures clearly establish that the trianionic form of **1** (**II′**) is six-coordinate and axially ligated by deprotonated solvent. In contrast, the preponderance of evidence on the EC-type complexes suggests a five-coordinate complex deprotonated at both coordinated N's.

(16) Nugent, W. A.; Mayer, J. M. *Metal-Ligand Multiple Bonds*; Wiley & Sons: New York, 1988; p 118.

Conclusions

Although the coordination environments are similar, ReO(NS)$_2$ and ReO(N_2S_2), the presence of the additional chelate ring in the LL-EC and DD-TMEC complexes clearly alters the solution chemistry compared to the D-pen complex. We presented clear evidence that in both water and methanol the dianionic (doubly deprotonated) form of **1** exists as a mixture of *anti*-carboxyl ligated and deligated forms. For the EC-type complexes, the only related dianionic species readily detected is carboxyl deligated. Thus, the ethylene chelate ring favors deligation in the EC-type complexes. Furthermore, the rate of the ligation/deligation process is faster for the EC-type complexes because the NMR signals are broad compared to the sharp signals always observed for all forms of **1**.

The acid−base titration demonstrated that the forms at the highest pH for the ReO(N_2S_2) and ReO(NS)$_2$ systems both require consumption of 3 equiv of base. Consumption of the second mole of base occurs at a much higher pH for the D-pen than for the EC-type complexes. The ReO(*anti*-D-penH$_3$-*N*,*S*,*O*)(*syn*-D-penH$_2$-*N*,*S*) complex exists essentially in one form near physiological pH, whereas the EC-type complexes are mixtures.[9]

The differences in carboxyl ligation and, possibly, coordination number between the D-pen- and EC-type complexes appear to be related to the facility of NH deprotonation. Deprotonated nitrogens are better donors, and deprotonation will favor lower coordination numbers. It is likely that the dianionic EC complexes are five-coordinate since, at the low pH of deprotonation of this type of complex, OH^- concentration is low. At higher pH, the second NH deprotonation of EC-type complexes occurs, disfavoring axial ligation by OH^-. Thus, there is no facile oxo group exchange mechanism available, accounting for the different spectral behavior at high pH of the D-pen- and EC-type complexes.

These results do have consequences in radiopharmaceutical design: they suggest that if a *syn* or *anti* configuration is to be maintained, the N_2S_2 ligand in its protonation state under physiological conditions must be electron rich enough to disfavor hydroxo group coordination. The chelate ring can alter the NH pK_a, perhaps lowering the pK_a into the physiological range, leading to a mixture of forms. In theory, the presence of only one form should lead to the most useful type of radiopharmaceutical, provided that form has a desirable biodistribution.

Acknowledgment. This work was supported by the National Institutes of Health (Grant No. DK38842). We thank the NIH and NSF for supporting the purchase of instruments.

IC950992N